

Journal of Visualized Experiments

Nanoscale Characterization of Liquid-Solid Interfaces by Coupling Cryo-Focused Ion Beam Milling with Scanning Electron Microscopy and Spectroscopy --Manuscript Draft--

Article Type:	Invited Methods Collection - JoVE Produced Video
Manuscript Number:	JoVE61955R1
Full Title:	Nanoscale Characterization of Liquid-Solid Interfaces by Coupling Cryo-Focused Ion Beam Milling with Scanning Electron Microscopy and Spectroscopy
Corresponding Author:	Lena F. Kourkoutis Cornell University Ithaca, NY UNITED STATES
Corresponding Author's Institution:	Cornell University
Corresponding Author E-Mail:	lena.f.kourkoutis@cornell.edu
Order of Authors:	Taylor Moon Lena F. Kourkoutis
Additional Information:	
Question	Response
Please specify the section of the submitted manuscript.	Engineering
Please indicate whether this article will be Standard Access or Open Access.	Standard Access (US\$2,400)
Please indicate the city, state/province, and country where this article will be filmed . Please do not use abbreviations.	Ithaca, NY, USA
Please confirm that you have read and agree to the terms and conditions of the author license agreement that applies below:	I agree to the Author License Agreement
Please provide any comments to the journal here.	

TITLE

Nanoscale Characterization of Liquid-Solid Interfaces by Coupling Cryo-Focused Ion Beam Milling with Scanning Electron Microscopy and Spectroscopy

AUTHORS AND AFFILIATIONS

Taylor Moon¹, Lena F. Kourkoutis^{1,2}

¹School of Applied and Engineering Physics, Cornell University, Ithaca, New York

²Kavli Institute at Cornell for Nanoscale Science, Ithaca, New York

Email address of co-author:

Taylor Moon (tbm46@cornell.edu)

Corresponding author:

Lena F. Kourkoutis (lena.f.kourkoutis@cornell.edu)

KEYWORDS

cryogenic FIB, cryogenic SEM, energy dispersive x-ray spectroscopy, solid-liquid interfaces, energy storage devices

SUMMARY

Cryogenic Focused Ion Beam (FIB) and Scanning Electron Microscopy (SEM) techniques can provide key insights into the chemistry and morphology of intact solid-liquid interfaces. Methods for preparing high quality Energy Dispersive X-ray (EDX) spectroscopic maps of such interfaces are detailed, with a focus on energy storage devices.

ABSTRACT

Physical and chemical processes at solid-liquid interfaces play a crucial role in many natural and technological phenomena, including catalysis, solar energy and fuel generation, and electrochemical energy storage. Nanoscale characterization of such interfaces has recently been achieved using cryogenic electron microscopy, thereby providing a new path to advancing our fundamental understanding of interface processes.

This contribution provides a practical guide to mapping the structure and chemistry of solid-liquid interfaces in materials and devices using an integrated cryogenic electron microscopy approach. In this approach, we pair cryogenic sample preparation which allows stabilization of solid-liquid interfaces with cryogenic focused ion beam (cryo-FIB) milling to create cross-sections through these complex buried structures. Cryogenic scanning electron microscopy (cryo-SEM) techniques performed in a dual-beam FIB/SEM enable direct imaging as well as chemical mapping at the nanoscale. We discuss practical challenges, strategies to overcome them, as well as protocols for obtaining optimal results. While we focus in our discussion on interfaces in energy storage devices, the methods outlined are broadly applicable to a range of fields where solid-liquid interface play a key role.

INTRODUCTION

Interfaces between solids and liquids play a vital role in the function of energy materials such as batteries, fuel cells, and supercapacitors¹⁻³. While characterizing the chemistry and morphology of these interfaces could play a central role in improving functional devices, doing so has presented a substantial challenge^{1,3,4}. Liquids are incompatible with the high vacuum environments needed for many common characterization techniques, such as x-ray photoemission spectroscopy, scanning electron microscopy (SEM) and transmission electron microscopy². Historically, the solution has been to remove the liquid from the device, but this comes at the expense of potentially damaging delicate structures at the interface^{2,4} or modifying morphology³. In the case of batteries, especially those which employ highly reactive alkali metals, this physical damage is compounded by chemical degradation upon exposure to air⁵.

This paper describes cryo-SEM and focused ion beam (FIB) as a method for preserving and characterizing solid-liquid interfaces. Similar methods have been shown to preserve the structure of cells in biological samples⁶⁻⁸, energy devices^{5,9-12} and nanoscale corrosion reactions¹³⁻¹⁵. The crux of the technique is to vitrify the sample via plunge freezing in slush nitrogen prior to transfer into the microscope where it is placed onto a cryogenically cooled stage. Vitrification stabilizes the liquid in the vacuum of the microscope while avoiding the structural deformations associated with crystallization^{6,8}. Once in the microscope, a dual beam system allows nanoscale imaging with the electron beam, and preparation of cross-sections with the focused ion beam. Lastly, chemical characterization is enabled via Energy Dispersive X-ray (EDX) mapping. Altogether, cryo-SEM/FIB can preserve the native structure of a solid-liquid interface, create cross-sections, and provide both chemical and morphological characterization.

In addition to providing a general workflow for cryo-SEM and EDX mapping, this paper will describe a number of methods to mitigate artifacts from milling and imaging. Often vitrified liquids are delicate and insulating, making them prone to charging as well as beam damage⁸. While a number of techniques have been established to reduce these unwanted effects in specimens at room-temperature¹⁶⁻¹⁸, several have been modified for cryogenic applications. In particular, this procedure details application of conductive coatings, first a gold-palladium alloy, followed by a thicker platinum layer. Additionally, instructions are provided to help users identify charging when it occurs and adjust the electron beam conditions to mitigate the accumulation of charge. Lastly, although beam damage has many characteristics in common with charging, the two can occur independent of one another¹⁶, and guidelines are provided for minimizing beam damage during the steps where it is most likely.

While dual-beam SEM/FIB is not the only electron microscopy tool to have been adapted for cryogenic operation, it is particularly well-suited for this work. Often realistic devices like a battery are on the scale of several centimeters in size, while many of the features of interest are on the order of microns to nanometers, and the most meaningful information can be contained in the cross-section of the interface^{4,5,19}. Although techniques like Scanning Transmission Electron Microscopy (STEM) combined with Electron Energy Loss Spectroscopy (EELS) enable imaging and chemical mapping down to the atomic scale, they require extensive preparation to

make the sample sufficiently thin to be electron transparent, dramatically limiting throughput^{3,4,19-22}. Cryo-SEM, by contrast, allows for the rapid probing of interfaces in macroscopic devices, such as the anode of a lithium metal battery coin cell, albeit at a lower resolution of tens of nanometers. Ideally, a combined approach that leverages the advantages of both techniques is applied. Here, we focus on higher throughput cryogenic FIB/SEM techniques.

Lithium metal batteries were used as the primary test case for this work, and they demonstrate the broad utility of cryo-SEM techniques: they feature delicate structures of scientific interest^{4,5,9-12}, have broadly varying chemistry to be revealed via EDX², and cryogenic techniques are required to preserve the reactive lithium^{5,21}. In particular, the uneven lithium deposits known as dendrites, as well as the interfaces with the liquid electrolyte are preserved and can be imaged and mapped with EDX^{4,5,12}. Additionally, lithium typically would oxidize during preparation and form an alloy with gallium during milling, but the preserved electrolyte prevents oxidation and cryogenic temperatures mitigate reactions with gallium⁵. Many other systems (energy devices especially) feature similarly delicate structures, complex chemistries and reactive materials, so the success of cryo-SEM on the study of lithium metal batteries can be considered a promising indication that it is suitable for other materials as well.

The protocol uses a dual-beam FIB/SEM system fitted with a cryogenic stage, a cryogenic preparation chamber and a cryogenic transfer system, as detailed in the **Table of Materials**. For preparing the cryo-immobilized samples there is a workstation with a “slush pot,” which is a foam insulated pot that sits in a vacuum chamber in the station. The foam insulated dual pot slusher contains a primary nitrogen chamber and a secondary chamber which surrounds the former and reduces boiling in the main part of the pot. Once filled with nitrogen, a lid is placed over the pot and the whole system can be evacuated to form slush nitrogen. A transfer system featuring a small vacuum chamber is used to transfer the sample under vacuum to the preparation or “prep” chamber of the microscope. In the prep chamber the sample can be kept at -175 °C and sputter coated with a conductive layer, such as a gold-palladium alloy. Both the prep chamber and the SEM chamber feature a cryogenically cooled stage for holding the sample, and an anticontaminator to adsorb contaminants and to prevent ice buildup on the specimen. The whole system is cooled with nitrogen gas that flows through a heat exchanger submerged in liquid nitrogen, and then through the two cryo-stages and two anticontaminators of the system.

PROTOCOL

1. Prepare the sample and transfer into the SEM chamber

1.1. Set up the microscope

1.1.1. For systems that convert between room temperature and cryogenic equipment, install the cryo-SEM stage and anticontaminator according to the equipment manufacturer’s instructions and evacuate the SEM chamber.

1.1.2. Adjust the gas injection system (GIS) platinum source so that when inserted it sits approximately 5 mm further away from the sample surface compared to typical room temperature experiments. This position needs to be optimized for each system to ensure even coating of the sample surface. On the FIB used here, this is done by loosening a set screw on the side of the GIS source and rotating the collar 3 turns clockwise.

1.1.3. Set the GIS temperature to 28 °C, open the shutter and vent for 30 s at this temperature to clear out excess material. Do this at room temperature, as the organometallic will coat any cold surface.

1.1.4. Move the stage to the proper position for loading of the sample shuttle from the preparation chamber into the SEM (this will vary by system).

1.1.5. Allow the SEM chamber to evacuate for a minimum of 8 h, to establish a low enough vacuum (typically about 4E-6 Torr) to minimize ice contamination during the experiment.

1.2. Set up the cryogenic preparation station

1.2.1. Evacuate the vacuum isolated lines for 8 h prior to use.

1.2.2. Before cooling the microscope, flow dry nitrogen gas through the gas lines for about 15 min. This should be done at approximately 5 L/min, or the maximum flow rate of the system. This flushes moisture out of the system to mitigate the formation of ice in the lines upon cooling, which can impede the flow of gas.

1.2.3. While still flowing gas at the maximum flow rate, close off the valve for the vacuum isolated lines, then transfer the heat exchanger into the liquid nitrogen Dewar.

1.2.4. Set the temperature of the SEM and prep stages to -175 °C, and the temperature of the anticontaminators to -192 °C. Wait until all elements have reached the set temperature to proceed.

1.3. Vitrify the sample.

1.3.1. Fill the nitrogen dual pot slusher. Start by filling the main volume of the pot, then fill the volume surrounding it to reduce nitrogen bubbling. Continue adding more liquid nitrogen to each as needed until boiling stops.

1.3.2. Seal the slusher with the lid and start the slush pump. Continue pumping until the liquid nitrogen starts solidifying.

1.3.3. Start venting the slush pot. For air sensitive materials like lithium batteries, this is a good time to prepare the sample for plunge freezing.

1.3.4. Once the pressure is high enough to allow the pot to be opened, quickly but gently set the sample in the nitrogen, and wait at least until the boiling has ceased around the sample to proceed. Remove all tools from the liquid nitrogen at this point to reduce the chances of ice contamination.

1.3.5. If the slush pot is less than half full, add more liquid nitrogen.

1.3.6. Transfer the sample to the SEM shuttle. Place any tools needed to secure or transfer the sample in the liquid nitrogen pot and allow them to fully cool, i.e., wait at a minimum until the LN₂ stops boiling around each tool, before touching the sample or shuttle. Extended exposure to atmosphere, especially when humid, can cause ice crystals to form in the liquid nitrogen, so it is best to do this step quickly.

1.3.7. Attach the shuttle to the transfer rod. As with other tools, pre-cool the end of the rod in the LN₂ before touching the shuttle.

1.3.8. Pump on the slush pot and watch the pressure. Lift the sample up out of the liquid nitrogen and seal it off in the vacuum chamber of the transfer system just before the nitrogen starts to freeze. Typically, this can be done by lifting the shuttle up when the pressure is ~8 mbar.

1.3.9. Quickly transfer to the airlock of the prep chamber and pump on the transfer system. Open the transfer system's vacuum chamber as soon as the airlock pressure is low enough for this to be done without much force.

1.3.10. Once the prep chamber can be opened, quickly transfer the sample shuttle into the chamber and place on the cooled prep stage. Retract the transfer rod and close the airlock door.

1.3.11. At this point, a ~5-10 nm gold-palladium layer can be sputtered onto the sample surface to mitigate charging. Typical starting values are 10 mA for 10 s, though these parameters should be adjusted for each system. Alternatively, one can image the uncoated surface, assess the extent of charging, and transfer back into the prep chamber to sputter coat.

1.3.12. Re-open the airlock, connect the transfer rod and wait 1 min for the end of the rod to cool down. Then, open the valve to the main SEM chamber and transfer the sample shuttle as quickly and smoothly as possible onto the cooled SEM stage. Retract the transfer rod and store it under vacuum to prevent ice contamination in case it is needed again.

CAUTION: Liquid nitrogen can cause injury if exposed to skin. Handle with care while wearing the appropriate personal protective equipment. Do not place in a sealed container, as evaporation can cause pressure build-up.

2. Image the sample surface and locate features

NOTE: The time required to set up to start imaging is usually sufficient to allow the sample to reach thermal equilibrium on the cryo-stage, especially if both stages in the prep-chamber and the SEM chamber are cooled to the same temperature and the transfer time of the shuttle from one stage to the other is minimized.

2.1. Set the beam parameters prior to imaging, starting with a low voltage (~2kV) and moderate current (~0.84 nA). For especially delicate samples, users may want to reduce these values, and more robust samples may tolerate higher voltage and current.

2.2. Image the surface starting at low magnification (100x), focus and do any steps required by the instrument. For example, on the FIB user here, the measured working distance must be linked to the stage position. Assess the sample for changes in contrast or shape before focusing at higher magnifications to reduce charging.

2.3. Bring the sample to approximately eucentric height and take another relatively low magnification image (100-200x).

2.4. Select a sacrificial test region with the vitrified liquid and identify potential issues due to beam damage or charging. Start imaging at 100x magnification for 5 s, then increase the magnification to about 1,000x and image for another 5 s, then reduce the magnification to 100x, collect one image and pause the beam. If the region exposed at high magnification has changed contrast, the sample may be damaging or charging, and users should again consider adjusting the beam parameters or re-sputter coating. For a more detailed procedure see reference¹⁸.

2.5. Search the sample for the regions of interest. This process will vary considerably by sample and may require some experimentation. Features which extend significantly above the surrounding surface will likely cause the vitrified liquid to be similarly raised, while other features may be hidden.

2.5.1. If the features of interest cannot be located, an EDX map may help. With the sample still oriented normal to the electron beam, follow the EDX mapping procedure described in step 4.

2.6. As features of interest are located, save both low and high magnification images of the surface as well as the stage position.

2.7. Repeat to locate as many sites as desired.

2.8. Select a region to image first and align that area to eucentric height following the instrument's protocol.

2.9. Tilt the sample so the surface is normal to the direction of the platinum GIS needle, and insert the GIS needle. Warm it to 28 °C and open the valve for ~2.5 min, then retract the source. This should produce a uniform layer of uncured organometallic platinum, and the user can briefly

image the sample surface to confirm even coverage. The deposition time will vary between instruments and should be adjusted to ensure an even layer 1-2 μm thick.

2.10. Tilt the sample shuttle towards the FIB source and expose the organometallic platinum to a 30 kV ion beam at 2.8 nA, 800x magnification for 30 s. Image with the electron beam to verify that the surface is smooth and lacks any signs of charging.

3. Prepare cross-sections

3.1. Take a snapshot of the sample surface using the ion beam at 30kV and a lower bulk milling current (~ 2.8 nA), identify the feature of interest and measure out the rough placement of the cross-section. Trenches milled using about 2.8 nA can be placed 1 μm away from the final cross-section and should extend past either side of the feature of interest by a few microns. Side windows (see 3.2) should be placed with one edge roughly flush with the desired final cross-section.

3.2. Create a side window for x-rays prior to milling the main trenches to reduce redeposition.

3.2.1. Draw a **Regular Cross Section** rotated 90° relative to where the trench will be. Orientation will depend on the configuration of each EDX detector; place the shallow end of this trench towards the EDX detector. In the instrument software used here, this rotation is done by clicking the **Advanced** tab for the pattern and entering a rotation angle, measured counterclockwise.

3.2.2. Re-size the rotated pattern to maximize the number of x-rays to exit the cross-section's surface, nominally 10 μm square. The size will depend on the detector geometry, and often smaller windows will suffice. Users can expedite the procedure by determining the minimum size of this trench.

3.3. Create a **Regular Cross Section** just large enough to reveal the feature of interest. This can be done quickly by using a high current (~ 2.8 nA) to create one trench, lowering the current to clean up, or more slowly by working only at a lower current (~ 0.92 nA).

3.3.1. Take a snapshot of the sample surface using the ion beam at 30 kV and the desired current (see **Discussion** for selection of current). Identify the feature of interest and finalize the placement of the trench done in 3.1

3.3.1.1. The trench dimensions will vary by sample, but a typical size is $25 \mu\text{m} \times 20 \mu\text{m}$. Both dimensions must be large enough to allow the entire feature of interest to be visible; x will determine the width of the cross section, while y will limit how far down into the trench the electron beam can see. Ensure that there is 1 μm of material left between the edge of this trench and the desired final cross-section.

3.3.2. Set the z-depth to 1 μm with the milling application set to silicon and begin milling using the software, but regularly pause the process and image the cross-section using the electron beam, then resume milling as needed.

3.3.3. Repeat this process until the trench is much deeper than the feature of interest, typically 10-20 μm deep. Samples containing multiple materials will often have highly variable milling times and may need more or less time than the 1 μm depth setting will estimate. Record the amount of time needed to create the rough trench to guide the depth used in 3.4.

3.4. Create a final clean cross-section

3.4.1. Lower the ion beam current to approximately 0.92 nA and take a snapshot. Verify the location of the feature of interest: if step 3.1.3 was done correctly, there will be about 1 μm of material remaining to be milled away.

3.4.2. Draw a **Cleaning Cross Section** using the FIB software. Overlap this cleaning window with the pre-made trench by at least 1 μm to help mitigate redeposition.

3.4.3. Set the z-depth, using the observations from step 3.3.3 to determine the value. For example, if half of the time was used on a 1 μm depth, re-set the depth to 0.5 μm .

3.4.4. Let the cleaning cross section run uninterrupted. When finished, image the cleaned cross-section using the electron beam.

4. Perform EDX mapping

4.1. Select the appropriate beam conditions for the sample (see **Discussion** for details)

4.2. Orient the sample to maximize x-ray counts. Each instrument will have an ideal working height for EDX; ensure that the feature of interest is at this height. Tilt such that the incident electron beam is as close to normal to the surface of interest as possible.

4.3. Insert the EDX detector and determine the appropriate process time. For highly beam sensitive samples, it may be necessary to test these conditions on a sacrificial region of the sample prior to mapping the site of interest.

4.3.1. In the detector's software, go to **Microscope Setup** and start the electron beam image, then hit record. This will measure the count rate and dead time.

4.3.2. Record both the average dead time and count rate. The ideal dead time will vary between detectors, but for the Oxford X-max 80 typical values range between 15-25. Lower values will give better resolution, and higher values correspond to higher count rates.

4.3.3. If the deadtime needs to be adjusted, change the EDX time constant (also known as **Process Time**). A lower process time will give a lower deadtime, and vice versa. Repeat until the deadtime is in the desired range.

4.3.4. Confirm that the count rate is reasonable. Lower count rates (1,000 counts/s and lower) will require longer acquisition times, which increases the likelihood that maps will be distorted by sample drift. If the count rate is too low, consider increasing the beam current and voltage, or increasing the process time.

4.4. Once the detector conditions have been established, collect the electron beam image.

4.4.1. Go to **Image Setup** and select the bit depth and image resolution, typically 8 bit and either 512 x 448 or 1024 x 896.

4.4.2. Adjust the imaging conditions for the EDX software. Often the imaging conditions are calibrated differently in the EDX software than in the SEM's own software, and magnification, brightness and contrast will need to be adjusted accordingly. In INCA hit the record button on the site of interest window, adjust the image as needed, then **record** another **image, iterating as needed**.

4.5. Adjust the mapping setup in the EDX software.

4.5.1. Select the **X-ray Map resolution, Spectrum Range, Number of Channels, and the Map Dwell Time**. The resolution of the EDX map must be lower than the electron image (typically 256 x 224), and **the energy range can be as low as the beam energy used**. Typically, the maximum number of channels are used, and the dwell time is set to 400 μ s.

4.5.2. **In the EDX software, select the area to map over**. This can be done either by selecting the whole field of view, or by selecting a smaller region on the electron beam image which may expedite the process.

4.6. Start acquiring the EDX map. Allow this to run until a sufficient number of counts are collected (see the discussion below). In the elemental maps window, pre-processed maps are displayed, and if features start to blur during this process it is a sign the sample is either drifting or being damaged. In this case, consider stopping the map and using the SEM software to determine the problem.

4.7. **When the map is complete, save the EDX map as a data cube**, which is a 3D array with an axis for both spatial coordinates in the image, and an axis for energy.

REPRESENTATIVE RESULTS:

This method has been developed on a dual FIB/SEM system equipped with a commercially available cryogenic stage, anticontaminator, and preparation chamber. For details, see the table of materials. We have primarily tested this method on lithium metal batteries with a number of

different electrolytes, but the method is applicable to any solid-liquid interface that will endure the amount of dose applied during EDX mapping.

Figure 1 illustrates the various components of the cryogenic system used here: the slush pot (Fig. 1A) where samples are frozen, the transfer system (**Figure 1B**) featuring a vacuum chamber to store the shuttle in during transfer, the preparation or “prep” chamber (**Figure 1C,D**) where samples are sputter coated, and the SEM cryogenic stage itself (**Figure 1E**). **Figure 2** (adapted from Zachman, et al. 2020)⁵ compares milling of a bare lithium foil at 25 °C and -165 °C, highlighting how cooling to cryogenic temperatures can help preserve samples during FIB milling. For EDX experiments, the FIB milling geometry should be optimized and the position of the EDX detector should be taken into account as shown schematically in **Figure 3**. **Figure 3A** depicts the milling setup viewed from the direction of the ion beam: A main trench and side window are created first, with the side window rotated clockwise 270 degrees to produce the desired depth gradient with respect to the position of the EDX detector. Subsequently, a cleaning cross-section is milled (blue box in **Figure 3A**) to create the final face of the cross-section. The side window is milled at least 1 μm past the end of the original main trench so that the cleaning cross-section will be at least flush with the side of this trench. The milled side window establishes a line of sight from each point in the cross-section to the detector (**Figure 3B**).

In **Figure 4**, **Figure 5**, and **Figure 6**, we focus on one materials system: the initial deposition of lithium onto a lithium substrate connected to a stainless-steel current collector in a dioxolane (DOL)/dimethoxyethane (DME) electrolyte. First, we demonstrate in **Figure 4** the difference between a well-prepared cryo-immobilized sample and a poorly prepared one, both using the lithium metal battery as an example. Improper vitrification can lead to morphological changes as well as crystallization, while air exposure causes ice contamination. For **Figure 4**, both samples were nominally prepared according to the same procedure, however, brief exposure to air most likely resulted in surface reactions for the sample shown in **Figure 4B** possibly due to a thinner electrolyte layer on the surface of the lithium electrode. Screening of each sample after loading into the cryo-FIB helps identify potential issues due to the vitrification process. **Figure 5** shows the results of mapping a lithium deposit in 1,3-dioxolane/1,2-dimethoxyethane (DOL/DME) with non-optimal conditions (3 kV, 1.1 nA). The dark feature in the center of the cross-section in **Figure 5A** shows contrast variations, likely an indication of an initially well-preserved interface. Much of that detail is, however, lost due to radiation damage during mapping (**Figure 5B**). In contrast, **Figure 6** shows a map of dead lithium (chunks of lithium that are no longer connected to the electrode) embedded in vitrified electrolyte and the lithium substrate beneath it done at 2 kV and 0.84 nA, which preserved the morphology. Although some damage is still visible in **Figure 6B**, the extent is substantially reduced.

EDX mapping can also be used to localize buried structures. **Figure 7** (adapted from Zachman, 2016)¹⁹ demonstrates the use of EDX to locate iron oxide nanoparticles grown in a silica hydrogel. Large field of view scans allow identification of regions of interest (**Figure 7A,D**), while more localized scans (**Figure 7B,E**) can be used for site-specific milling (**Figure 7C,F**), in this case in preparation for a cryo-lift-out.

Standard safety procedures for handling cryogenics (namely liquid nitrogen and slush nitrogen) should be used when following this procedure, and lithium metal batteries should be handled with the appropriate personal protective equipment and disposed of safely.

FIGURE LEGENDS

Figure 1: Components of the cryogenic FIB/SEM system used. (A) The slush pot for initial sample preparation. The main portion and a reservoir under the foam insulation are filled with liquid nitrogen, which is converted into slush nitrogen by reducing the pressure above the liquid nitrogen using a vacuum pump. Samples are plunge frozen in the slush nitrogen and attached to the shuttle before the vertical dock is used to lift the shuttle out on the transfer arm. (B) The inside of the transfer system. A small airlock holds the shuttle under weak vacuum during transfer to the preparation chamber, and the arm itself (not shown) allows users to move the sample onto the cryogenically cooled stage. (C) An outside view of the preparation chamber, where samples can be sputter-coated prior to imaging. (D) A closeup of the cryo-stage in the preparation chamber. (E) The cryo-system inside the SEM chamber, featuring the stage and the anticontaminator.

Figure 2: Comparison of milling a lithium foil at room-temperature vs. cryogenic temperature. (A) A cross-section created by a regular cross-section at room temperature. The face of the cross-section is not smooth and additional material is present. This is likely a lithium-gallium alloy formed during milling with the gallium ion beam. (B) A trench milled using a cleaning cross section. The face is now clean, but redeposition in the trench is pronounced. (C) The same as (A) but done at -165°C . The face lacks the lithium-gallium alloy, and redeposition is reduced. (D) the same as (B) but performed at -165°C . The final trench and cross-section are extremely clean. Together this suggests that gallium ion-based FIB techniques are incompatible with lithium samples at room-temperature but are compatible at cryogenic temperatures. Adapted from Zachman, 2020⁵.

Figure 3: Setup of milling windows, including a side window for improved x-ray yield. (A) A schematic showing the key features of the milling process (placements are not exact). The main trench and side window are drawn showing the direction of increasing depth (indicated both by the labeled arrows and the gradient in shading), and the cleaning cross-section (blue) is shown overlapping partially with the main trench. The side window is aligned relative to the position of the EDX detector to allow for detection of x-rays generated from the entire cross-section. (B) A sketch demonstrating the benefit of the side window. As the electron probe scans the cross-section, electrons excite x-rays, which are measured by the EDX detector. Without a side window, shadow effects would cause parts of the cross-section (such as the bottom right here) to appear dark.

Figure 4: Results of improper vitrification and transfer. (A) A well-preserved lithium sample with a DOL/DME electrolyte. While deposits cause some three-dimensional variations, the cryo-immobilized electrolyte is generally smooth and uniform. (B) A representative result of a less well-preserved sample of the same system. The surface is far rougher, and deposits are not fully

covered by electrolyte, suggesting sample reactions may have occurred due to prolonged air exposure during the preparation.

Figure 5: EDX mapping of a lithium metal battery with reduced shadowing, but significant damage. (A) The electron beam image prior to EDX mapping at 3 kV and 1.1 nA. (B) the post-mapping image, showing damage of smaller structures. (C) The electron image corresponding to the mapped region. (D) carbon K- α elemental map with red lines indicating the shadowing. Within the side window, there is significant shadowing that would otherwise obscure the face of the cross-section. The side window was not perfectly aligned and slightly extends past the face of the cross-section, resulting in the limited shadowing visible in this region.

Figure 6: EDX mapping of dead lithium in a lithium metal battery with minimal damage and shadowing. (A) The electron beam image prior to EDX mapping at 2 kV and 0.84 nA with asterisks marking the dead lithium. (B) The post-mapping image, showing very little damage due to more optimized beam conditions. (C) The electron image corresponding to the mapped region. (D) Carbon K- α elemental map with red line indicating minor shadowing effects.

Figure 7: EDX mapping to identify buried features of interest. (A) SEM image of a silica hydrogel with embedded iron oxide nanoparticles. (B) A similar image recorded at higher magnification. (C) An SEM image of two trenches centered on an iron oxide nanoparticle, created in preparation for cryo-lift-out of a TEM lamella. (D,E) The EDX maps corresponding to (A, B). At higher magnification (E), it is possible to clearly distinguish several iron rich particles in the sample. By comparing with (B), it is possible to determine that one particle is embedded (indicated with an arrow) in the hydrogel, while others are not. (F) The EDX map of (C), showing clearly that the trenches are centered on the feature of interest. Adapted from Zachman, 2016¹⁹.

DISCUSSION

The cryogenic preparation method described here is important and must be done correctly for the chemistry and morphology to be preserved⁸. The foremost concern is freezing the sample quickly since this is what allows the liquid to be vitrified⁸. If the sample cools too slowly, liquids may crystallize resulting in a change in morphology⁶. To prevent crystallization, slush nitrogen is used in this procedure, as it reduces the Leidenfrost effect and accelerates cooling compared to liquid nitrogen^{8,23,24}. We also note that compared to aqueous solutions many organic liquids require significantly lower cooling rates for vitrification^{25,26}, which is beneficial for freezing of thicker organic electrolyte layers. Other cryogenics such as liquid ethane or propane are often used in other areas⁸, however, organic cryogenics can dissolve organic electrolytes which can give rise to artifacts^{23,24}. Slush nitrogen does not interact with organic liquids and is therefore the cryogen of choice here. To ensure rapid cooling, it is also important to eliminate extraneous mass from the sample during plunging to reduce heat capacity. Some samples (e.g., lithium metal anodes) may need to be attached to a holder like an aluminum stub for support during plunging, but if possible, it is better to attach the sample to the holder under liquid nitrogen, after it is properly frozen. Lastly, the cryogenic temperatures make the sample prone to ice contamination. Therefore, it is important that the sample is kept under vacuum during transfer from the slush pot to the prep chamber.

Sample charging and radiation damage can be a significant challenge even when operating at cryogenic temperatures, requiring protective coatings and careful selection of beam parameters. The primary methods for reducing these effects in this procedure focus on reducing beam voltage and providing paths for accumulated charge to dissipate. Reducing the beam voltage presents a tradeoff: while lower voltages typically reduce charge accumulation, the depth of beam damage, and the heat transferred into the sample^{16,17}, they also reduce count rates for EDX and the image resolution¹⁸. It is therefore recommended to determine the effect of each voltage available and utilize the highest voltage that does not damage the sample. To dissipate charge, the sample is coated initially with a thin (5-10 nm) conductive layer, such as gold-palladium and then a layer of platinum approximately one micron thick. FIB systems typically use an organometallic platinum gas to carry the platinum to the surface of the sample. Under cryogenic conditions this precursor condenses on the cold sample surface to form a non-conductive platinum-containing organic compound²⁷. A curing process during which the layer is exposed to the ion beam then releases the organic component, allowing a conductive platinum layer to form. This step is critical for high-quality results as the platinum both dissipates charge and mitigates gallium implantation^{13,27}. Orienting the sample so that the surface is normal to the GIS source is the best way to get a continuous layer, and the exact position will need to be adjusted for each system. Lastly, the sample must have a continuous conductive path to ground for excess charge to dissipate, provided by a grounding wire connected to the stage. In addition to this grounding wire, the sample itself must have good conductivity to the shuttle for charge to dissipate.

The procedure for preparing cross-sections is only slightly modified from the standard method for room-temperature FIB work¹⁷. The primary modification is the addition of a side window to allow more x-rays to escape the trench. Without this window, one side of the trench will produce a shadow over the face of the cross-section in EDX maps. Although one could ensure the shadow does not obscure the feature of interest by simply extending one side of the trench, doing so would take longer than the method described here. Using a regular cross section rotated 90 degrees relative to the main trench creates a direct path from every point in the cross-section to the x-ray detector while removing the minimum amount of material. Users should consider the orientation of the x-ray detector in the FIB chamber and place the side window accordingly. The other major modification is the use of lower milling currents to preserve the interface. At room temperature, it is common to use higher ion beam currents (~9.3 nA) to mill away the majority of the trenches, then reduce the current to mill a smaller window before cleaning¹⁷. Here, it is recommended that the higher currents are used with caution, as it damages many vitrified samples.

A major limitation of EDX mapping in the cryo-FIB is the large number of counts required relative to the count rates achievable under typical conditions. Statistically significant maps require over 100 counts per pixel, or on the order of 6 million counts for a 256 x 256 map¹⁷. Given that the beam conditions appropriate for cryogenic samples frequently give count rates as low as 1,000 counts per second, users can expect maps to take anywhere from several minutes to an hour. This time not only reduces throughput, but also increases the sensitivity to sample drift, which limits the quality of the maps. It is therefore worthwhile to optimize the count rate. The first step

in doing so will be to ensure that the sample is at the optimum working height for the detector in the system being used. Next, the beam parameters should be balanced to maximize x-ray yield without damaging the sample. Within the range of beam voltages considered here (2-5 keV), the count rate will increase with both beam voltage and current¹⁷, and the highest values that will not produce significant damage or charging should be used. However, the sample frequently constrains the beam conditions significantly, and it becomes even more important to optimize the EDX detector's conditions. The primary parameter that will need to be adjusted is known as "process time" in the Oxford Inca software (also known as a "time constant"), and its effect on the so-called dead time of the detector¹⁷. The dead time is a simple parameter, defined as:

$$\text{Dead time}(\%) = \frac{(\text{Input count rate} - \text{output count rate})}{\text{Input count rate}} \times 100,$$

where the input count rate refers to the number of electrons incident on the detector, and the output count rate refers to the number that the detector counts as signal¹⁷. The process time is a complex parameter, representing the time used to average the incoming signal. Longer process times represent more time averaging the signal, and therefore a higher process time will lead to a higher dead time. A low dead time represents the majority of x-rays being included, and for this application that is desirable, but it comes at the cost of resolution¹⁷. Typically process time is adjusted to give a dead time between 15 and 20%, but at lower voltages and currents it may not be possible to significantly improve the dead time.

Cryogenic FIB/SEM with EDX provides one of the few ways to probe both the chemistry and morphology of an intact solid-liquid interface. Methods such as Fourier-Transform Infrared Spectroscopy (FTIR), Raman Spectroscopy and XPS are commonly used to explore chemistry of batteries, but lack spatial resolution provided by EDX mapping². XPS is typically a destructive technique, but cryogenic temperatures have also been employed to preserve intact solid-liquid interfaces during XPS analysis²⁸. Morphology is often characterized using SEM, light microscopy, Atomic Force Microscopy (AFM) and Scanning Probe Microscopy (SPM)². Cryo-TEM/STEM has shown superior spatial resolution^{4,9,11,21,22} with more information-rich chemical mapping provided by EELS⁴ but is a low throughput technique. Samples must be restrictively thin, requiring either highly specific sample design (such as lithium grown on a TEM grid^{9,11,21,22}) or prepared from a macroscopic sample using cryo-FIB lift-out^{4,19}. Recently, Schreiber, et al.¹³ described using cryo-FIB methods to prepare intact solid-liquid interfaces for study via atom probe tomography. However, this procedure is relatively low-throughput and predominantly looks at the nanoscale^{13,14}, making its applications distinct from cryo-SEM EDX mapping.

Despite the notable advantages of this method, it is not without limitations. As discussed previously, much care must be taken to prevent damage to the sample during EDX mapping, and a small amount of damage may prove unavoidable. The specific equipment used in development of this work has limitations of its own. While detection of lithium by EDX is possible²⁹, it requires the use of a detector specifically optimized for low energy x-rays which was not done in this work. More sensitive detector will also improve the x-ray collection efficiency and thereby reduce the required electron dose for EDX mapping. Next, the technique is not immediately compatible with

all sample geometries. For example, some battery samples tend to feature a thick electrolyte layer (30-100 μm) upon freezing which will require impractically long milling times when using a standard gallium ion FIB. Often slight modifications can be made to overcome this limitation. We have found that the electrolyte thickness can be reduced by switching from an O-ring separator to a membrane separator. However, the impacts of such modifications will vary between samples and should be done with careful consideration. Lastly, the Quorum cryogenic stage is an early model which lacks rotation about the vertical axis, limiting observations to a set orientation. Enabling stage rotation while maintaining stable a cryogenic sample temperature would improve the ease of use but is unlikely to significantly improve the quality of the results or expand the scope of the technique.

ACKNOWLEDGEMENTS

We greatly acknowledge the contributions by Shuang-Yan Lang and Héctor D. Abruña who provided samples for our research. This work was supported by the National Science Foundation (NSF) (DMR-1654596) and made use of the Cornell Center for Materials Research Facilities supported by the NSF under Award Number DMR-1719875.

DISCLOSURES

The authors have nothing to disclose.

REFERENCES

1. Schmickler, W., Santos, E. *Interfacial Electrochemistry*. Springer Berlin Heidelberg. Berlin, Heidelberg. (2010).
2. Cheng, X. -B., Zhang, R., Zhao, C. -Z., Wei, F., Zhang, J. -G., Zhang, Q. A review of solid electrolyte interphases on lithium metal anode. *Advanced Science*. **3** (3), 1500213 (2016).
3. Allen, F. I., et al. Morphology of hydrated as-cast Nafion revealed through cryo electron tomography. *ACS Macro Letters*. **4** (1), 1–5 (2015).
4. Zachman, M. J., Tu, Z., Choudhury, S., Archer, L. A., Kourkoutis, L. F. Cryo-STEM mapping of solid–liquid interfaces and dendrites in lithium-metal batteries. *Nature*. **560** (7718), 345–349 (2018).
5. Zachman, M. J., Tu, Z., Archer, L. A., Kourkoutis, L. F. Nanoscale elemental mapping of intact solid–liquid interfaces and reactive materials in energy devices enabled by cryo-FIB/SEM. *ACS Energy Letters*. **5** (4), 1224–1232 (2020).
6. Dubochet, J. The physics of rapid cooling and its implications for cryoimmobilization of cells. *Methods in Cell Biology*. **79**, 7–21 (2007).
7. Kourkoutis, L. F., Plitzko, J. M., Baumeister, W. Electron microscopy of biological materials at the nanometer scale. *Annual Review of Materials Research*. **42** (1), 33–58 (2012).
8. Dubochet, J. et al. Cryo-electron microscopy of vitrified specimens. *Quarterly Reviews of Biophysics*. **21** (2), 129–228 (1988).
9. Wang, X., Li, Y., Meng, Y.S. Cryogenic electron microscopy for characterizing and diagnosing batteries. *Joule*. **2** (11), 2225–2234 (2018).

10. Zachman, M. J., de Jonge, N., Fischer, R., Jungjohann, K. L., Perea, D. E. Cryogenic specimens for nanoscale characterization of solid–liquid interfaces. *MRS Bulletin*. **44** (12), 949–955 (2019).
11. Li, Y., Huang, W., Li, Y., Chiu, W., Cui, Y. Opportunities for cryogenic electron microscopy in materials science and nanoscience. *ACS Nano*. acsnano.0c05020 (2020).
12. Lee, J. Z. et al. Cryogenic focused ion beam characterization of lithium metal anodes. *ACS Energy Letters*. **4** (2), 489–493 (2019).
13. Schreiber, D. K., Perea, D. E., Ryan, J. V., Evans, J. E., Vienna, J. D. A method for site-specific and cryogenic specimen fabrication of liquid/solid interfaces for atom probe tomography. *Ultramicroscopy*. **194**, 89–99 (2018).
14. Perea, D. E. et al. Tomographic mapping of the nanoscale water-filled pore structure in corroded borosilicate glass. *NPJ Materials Degradation*. **4** (1), 1–7 (2020).
15. Li, T. et al. Cryo-based structural characterization and growth model of salt film on metal. *Corrosion Science*. **174**, 108812 (2020).
16. Egerton, R. F., Li, P., Malac, M. Radiation damage in the TEM and SEM. *Micron*. **35** (6), 399–409 (2004).
17. Goldstein, J. I. et al. *Scanning Electron Microscopy and X-Ray Microanalysis*. Springer New York. New York, NY. (2018).
18. Joy, D. C., Joy, C. Low voltage scanning electron microscopy. *Micron*. **27** (3–4), 247–263 (1996).
19. Zachman, M. J., Asenath-Smith, E., Estroff, L. A., Kourkoutis, L. F. site-specific preparation of intact solid–liquid interfaces by label-free *in situ* localization and cryo-focused ion beam lift-out. *Microscopy and Microanalysis*. **22** (6), 1338–1349 (2016).
20. Padgett, E. et al. Editors’ Choice—Connecting fuel cell catalyst nanostructure and accessibility using quantitative cryo-STEM tomography. *Journal of The Electrochemical Society*. **165** (3), F173–F180 (2018).
21. Li, Y. et al. Atomic structure of sensitive battery materials and interfaces revealed by cryo–electron microscopy. *Science*. **358** (6362), 506–510 (2017).
22. Wang, J. et al. Improving cyclability of Li metal batteries at elevated temperatures and its origin revealed by cryo-electron microscopy. *Nature Energy*. **4** (8), 664–670 (2019).
23. Oostergetel, G. T., Esselink, F. J., Hadzioannou, G. Cryo-electron microscopy of block copolymers in an organic solvent. *Langmuir*. **11** (10), 3721–3724 (1995).
24. Echlin, P. *Low-Temperature Microscopy and Analysis*. Springer US. Boston, MA. (1992).
25. Koifman, N., Schnabel-Lubovsky, M., Talmon, Y. Nanostructure formation in the lecithin/isooctane/water system. *The Journal of Physical Chemistry B*. **117** (32), 9558–9567 (2013).
26. Hayles, M. F., Stokes, D. J., Phifer, D., Findlay, K. C. A technique for improved focused ion beam milling of cryo-prepared life science specimens. *Journal of Microscopy*. **226** (3), 263–269 (2007).
27. Shchukarev, A., Ramstedt, M. Cryo-XPS: probing intact interfaces in nature and life. *Surface and Interface Analysis*. **49** (4), 349–356 (2017).
28. Hovington, P. et al. Can we detect Li K X-ray in lithium compounds using energy dispersive spectroscopy? *Scanning*. **38** (6), 571–578 (2016).

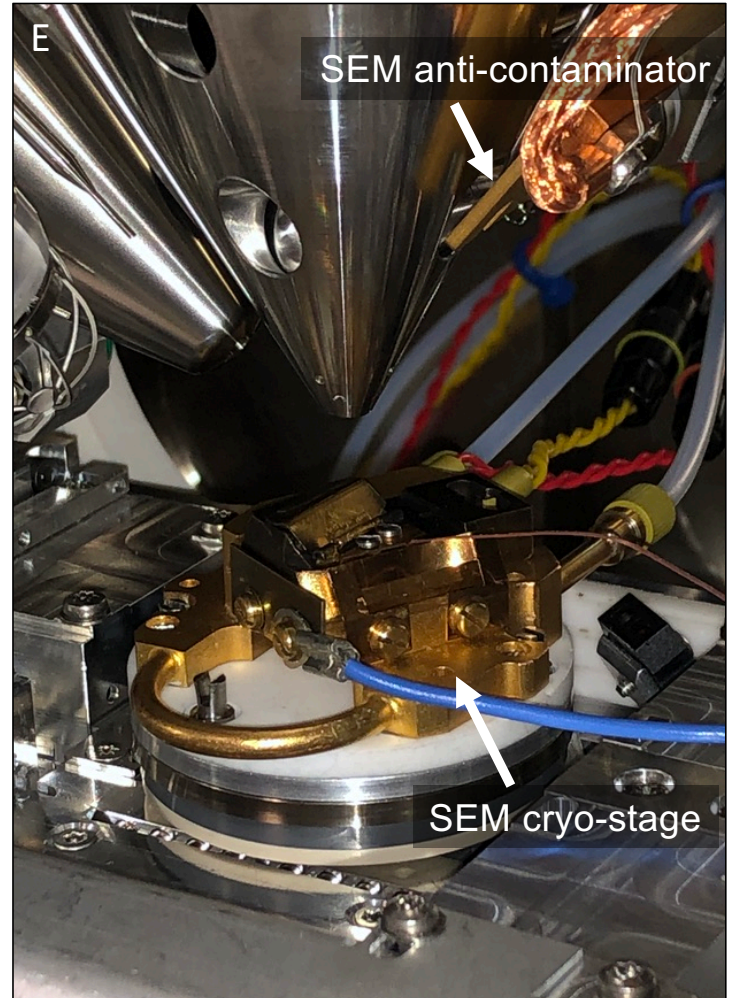
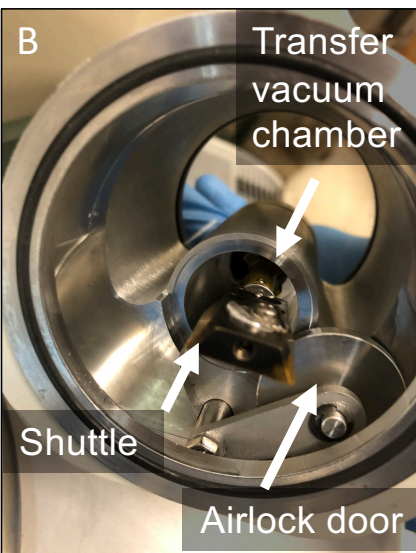
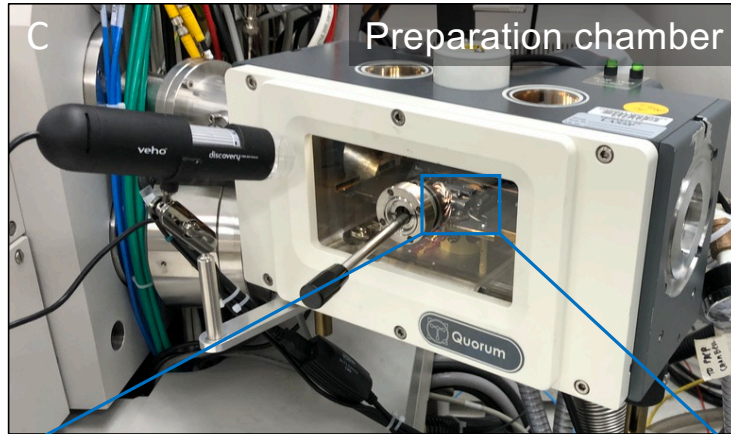
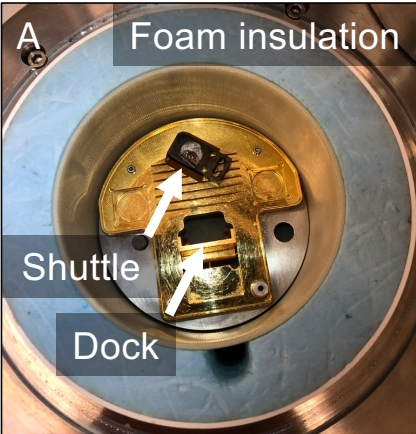
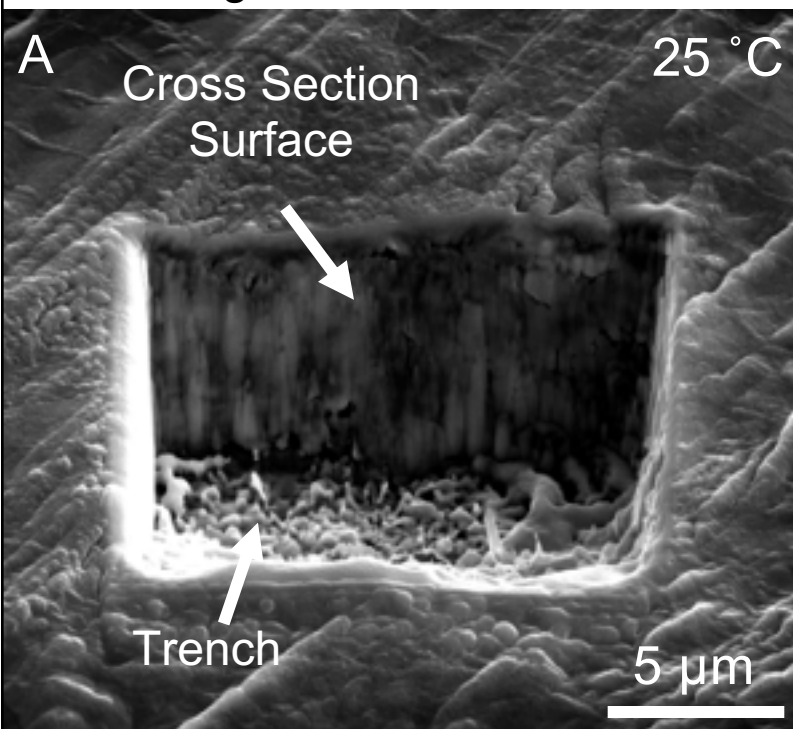


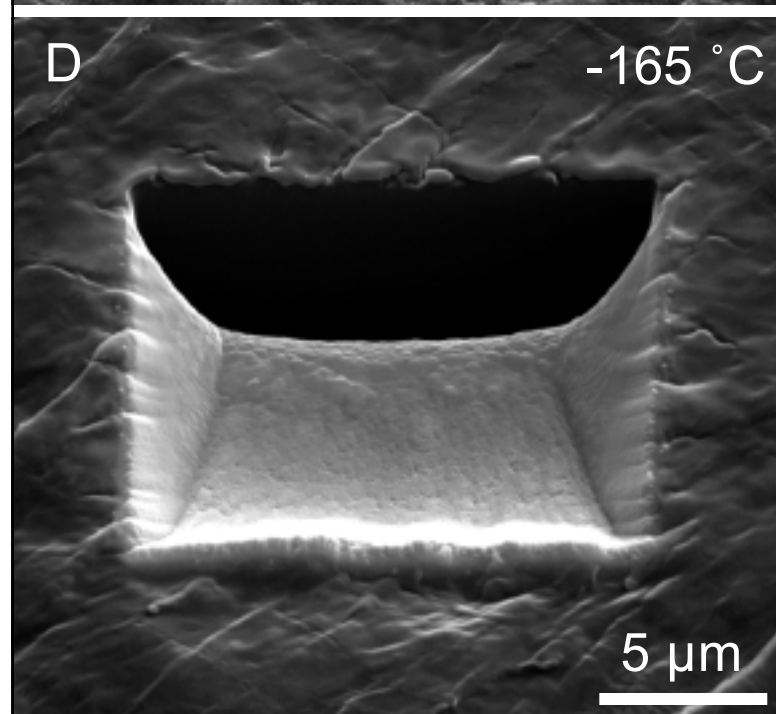
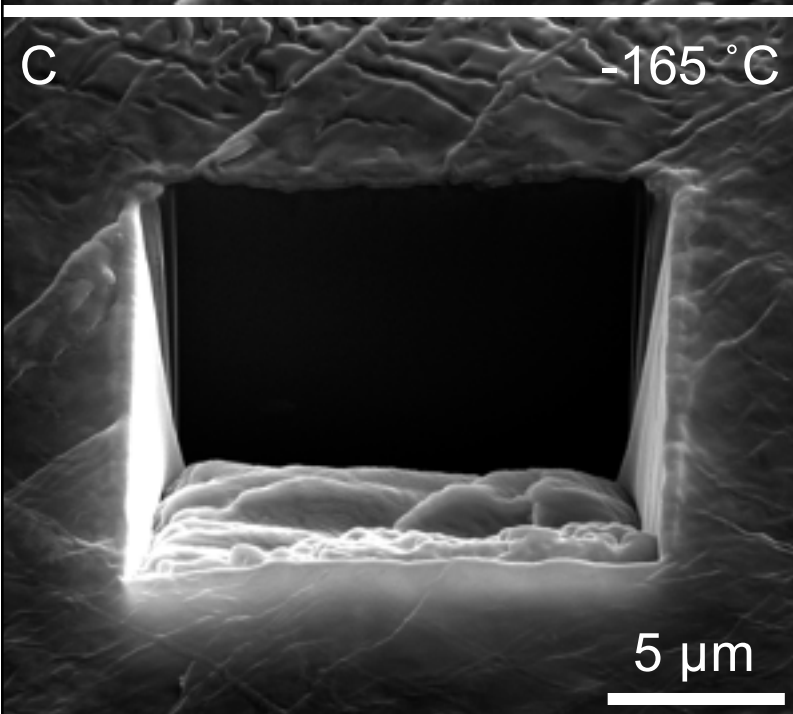
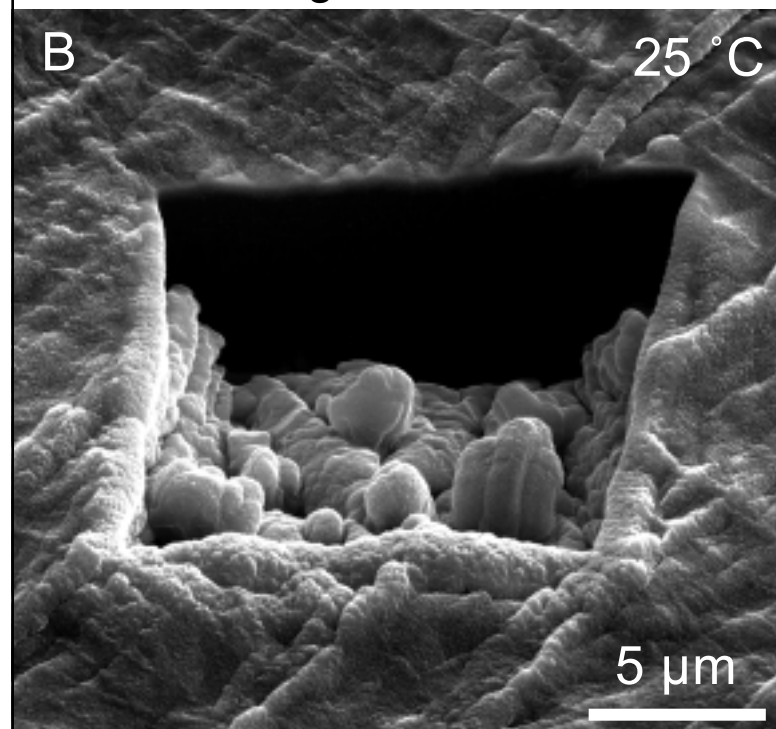
Figure 2

[Click here to access/download;Figure;Figure 2.pdf](#)

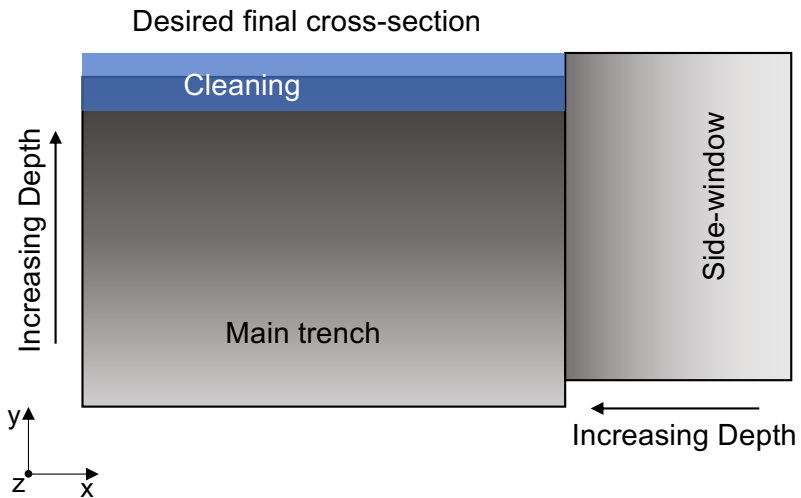
Regular Cross Section



Cleaning Cross Section



A



B

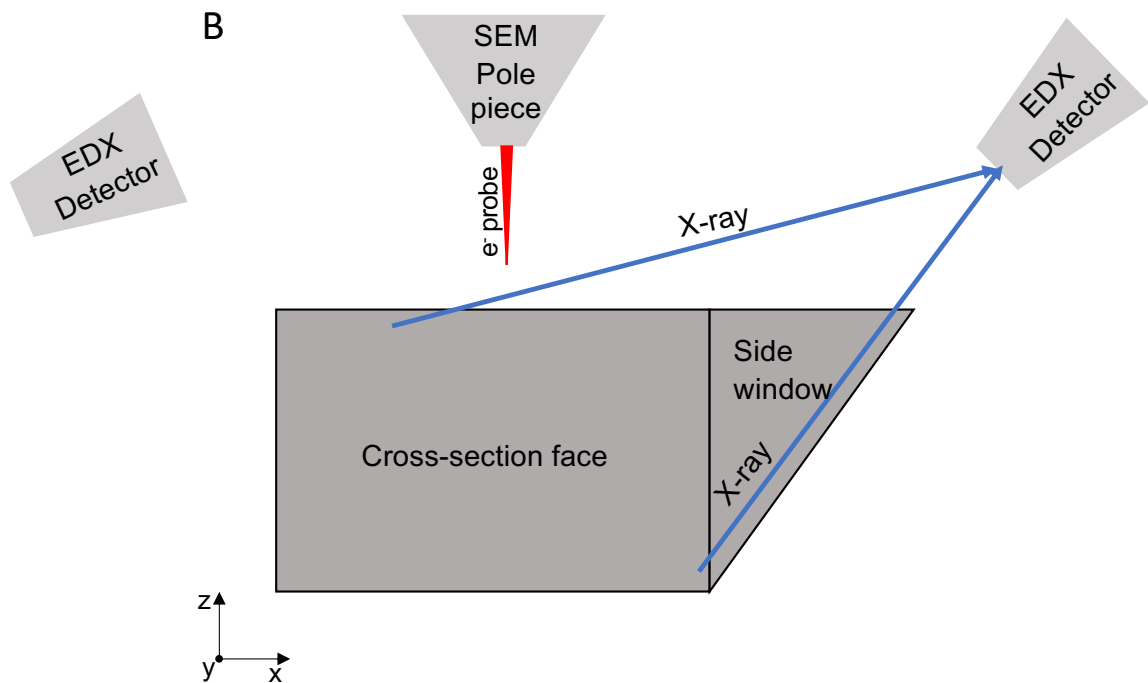
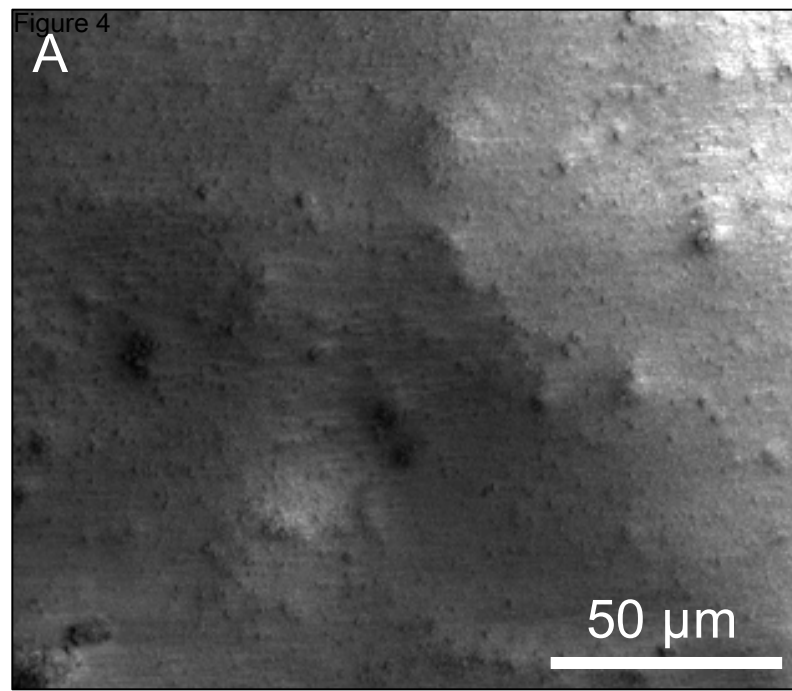
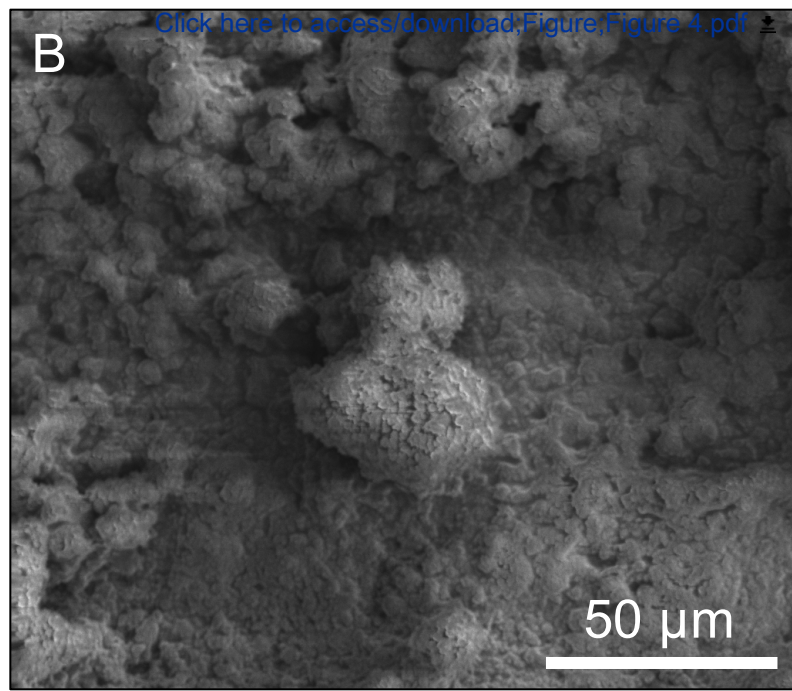


Figure 4

A



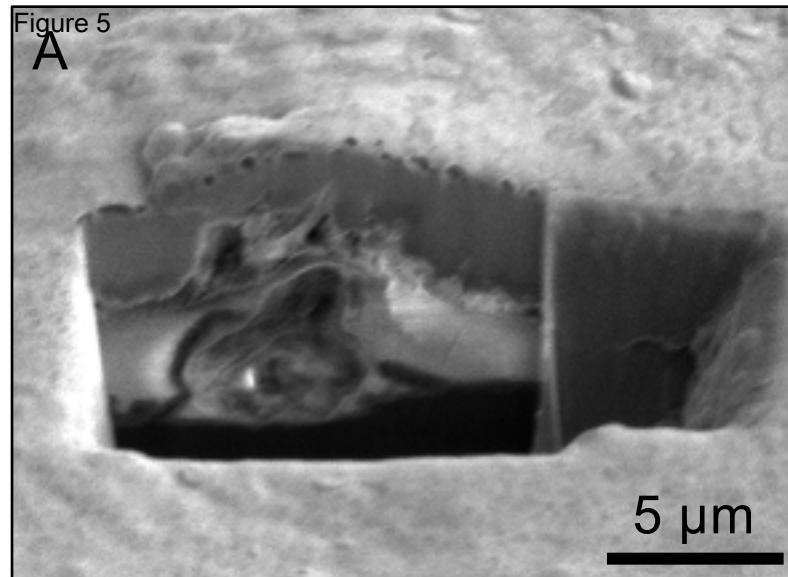
B



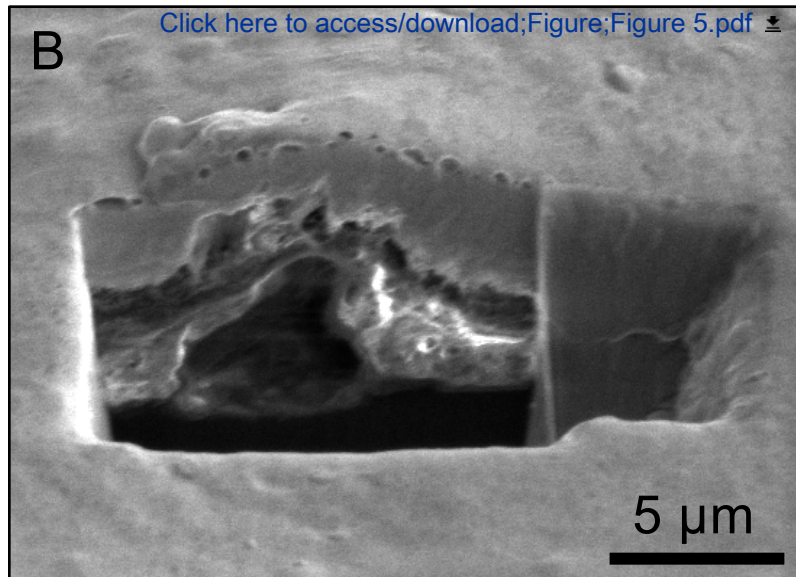
[Click here to access/download,Figure;Figure 4.pdf](#)

Figure 5

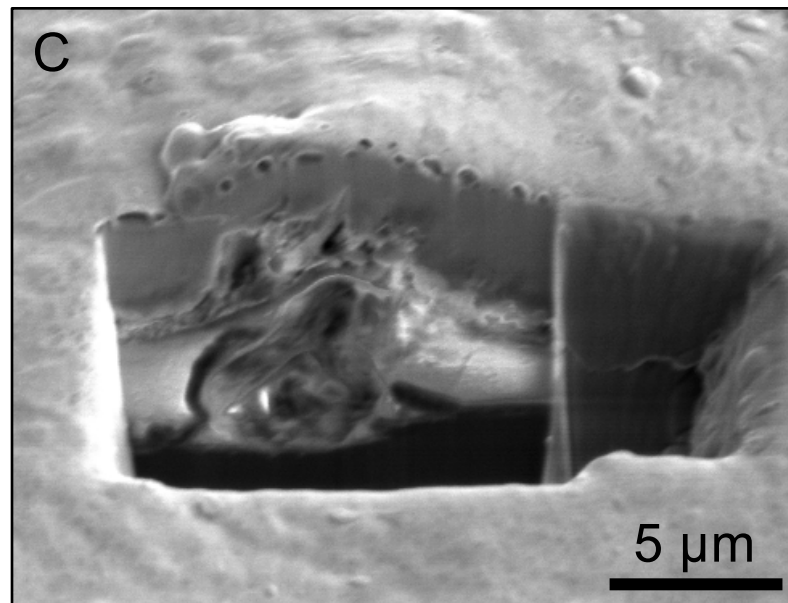
A



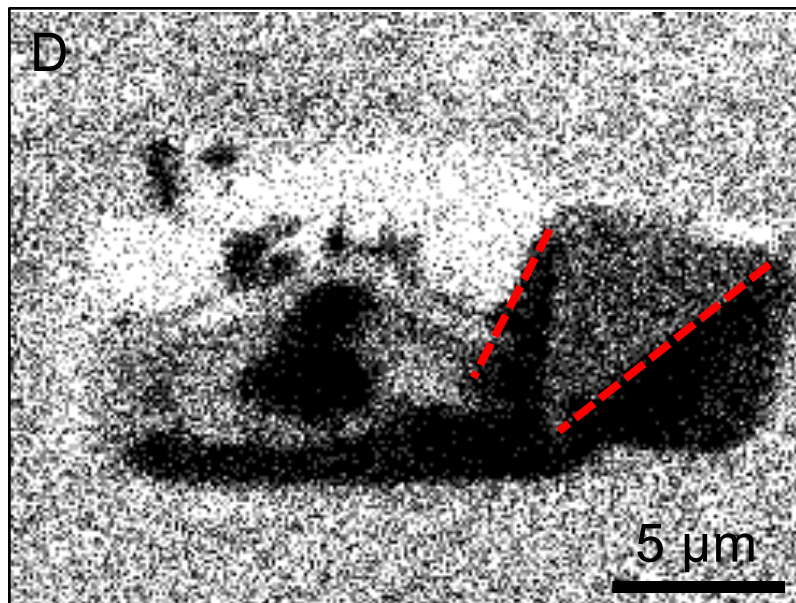
B

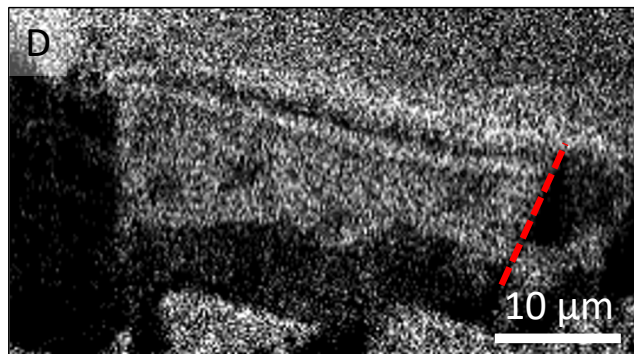
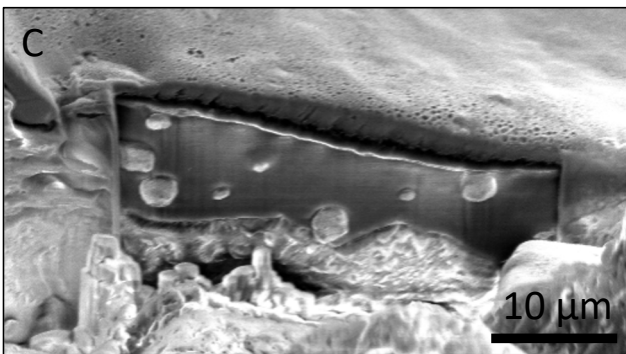
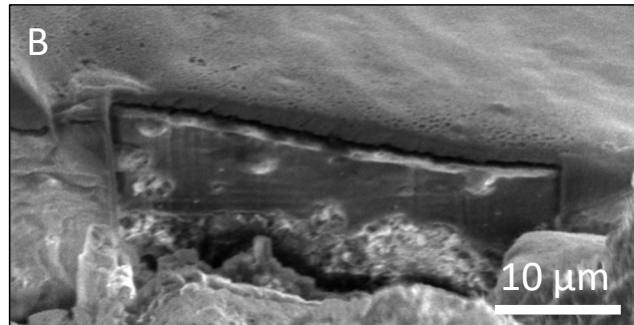
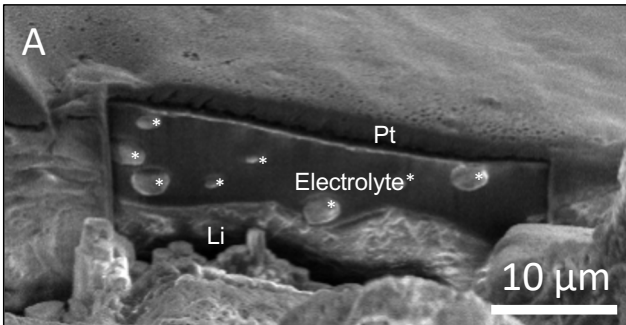


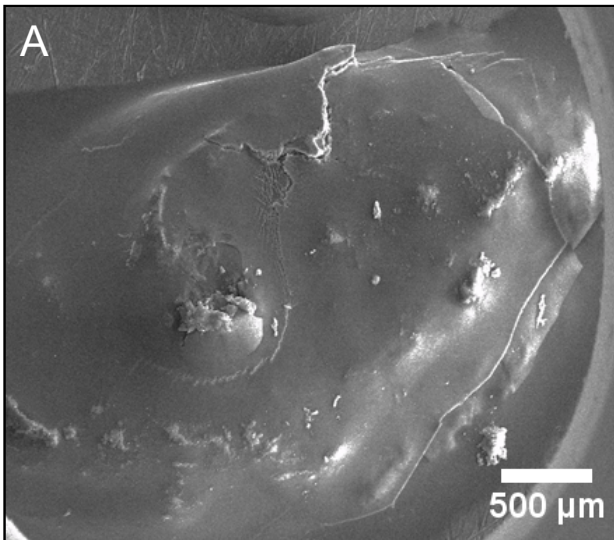
C



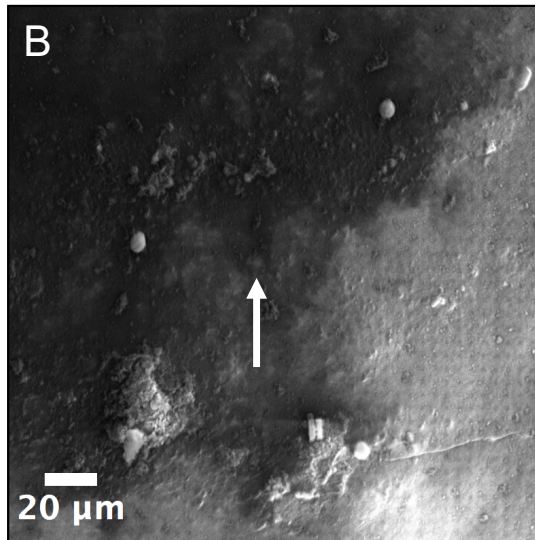
D



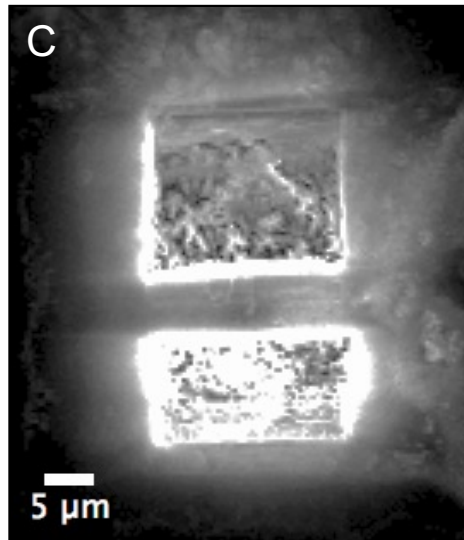




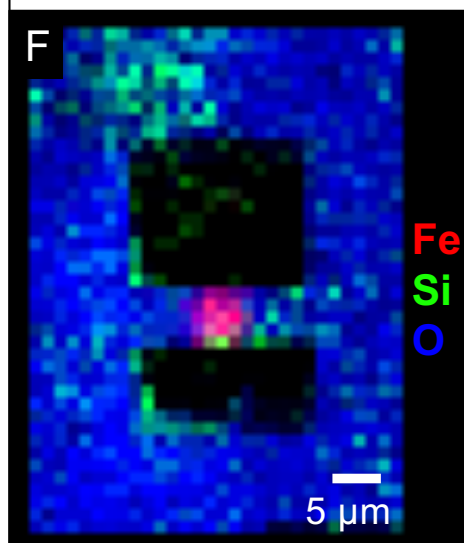
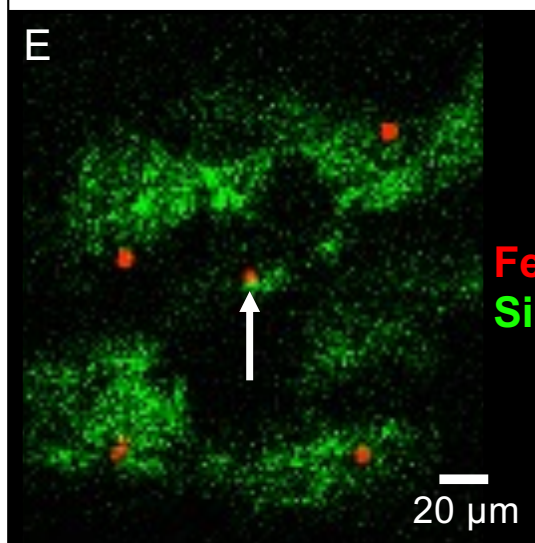
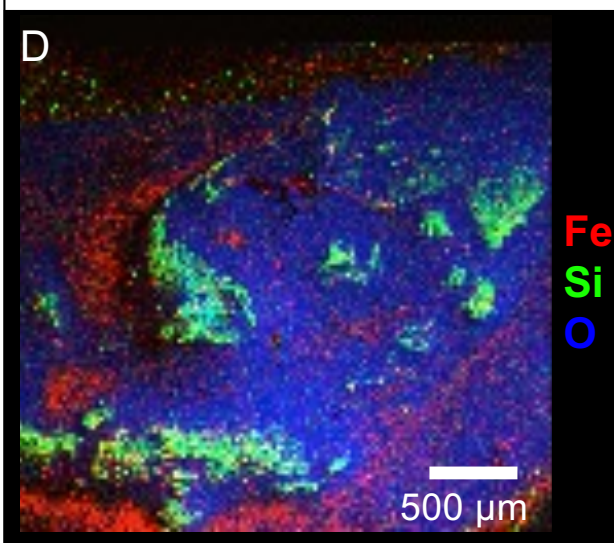
Region of Interest Identification



Subsurface Particle Localization



Site-Specific Milling



Name of Material/ Equipment	Company	Catalog Number
INCA EDS	Oxford instruments	
PP3010T Cryo-preparation system	Quorum Technologies, Inc.	
Strata 400 DualBeam System	FEI Co. (now Thermo Fisher Scientific)	
X-Max 80	Oxford Instruments	
xT Microscope Control	FEI Co. (now Thermo Fisher Scientific)	

Comments/Description

Control software for X-max 80

FIB/SEM cryogenic preparation system. Includes pumping station, transfer rod system, preparation (prep) chamber, cryogenic stages, sample shuttles

Dual beam FIB/SEM
80mm² EDX detector

Software for controlling FEI Strata

Point-by-point Response to Editorial Comments:

Editorial comments:

Changes to be made by the Author(s):

1. Please take this opportunity to thoroughly proofread the manuscript to ensure that there are no spelling or grammar issues. Please refer to the instructions for authors.

We have proofread the manuscript and the re-submission should be corrected.

2. 3.2: Please explain how and where to create a side window for x-rays.

We have added a figure for this purpose, namely figure 3 in the new draft. More detail of the edits is provided in the response to reviewer 3.

3. 4.5: Where is the SmartMap setup; which software: SEM or EDX?

This step now reads: "Adjust the SmartMap setup in the EDX software"

4. Please cite all figures in order.

This has been corrected.

5. Please consider showing images (or in the video) the improvement in the map by modifying the process as indicated in the representative results (lines 322-324).

We replaced one figure (number 4 in the previous draft) with one that represents more clearly those improvements including shadowing that has almost completely been avoided and reduced beam damage by mapping at a lower voltage of 2kV.

6. Please obtain explicit copyright permission to reuse any figures from a previous publication. Explicit permission can be expressed in the form of a letter from the editor or a link to the editorial policy that allows re-prints. Please upload this information as a .doc or .docx file to your Editorial Manager account. The Figure must be cited appropriately in Figure Legend, i.e. "This figure has been modified from [citation]."

The explicit copyright permissions for reuse of figures have been obtained prior to our initial submission. We have now included the official notifications and updated the citation in the figure legends.

7. Line 428: Please avoid the use of contractions (use "does not" instead of "doesn't").

This has been fixed throughout.

8. As we are a methods journal, please revise the Discussion (3-6 paragraphs) to also include the following in detail with citations:

- a) Any limitations of the technique
- d) The significance with respect to existing methods
- e) Any future applications of the technique

Please refer to lines 678-711 in the revised draft. Two paragraphs were added to address these concerns, and the first paragraph from the original discussion section was eliminated and merged into the others to meet the 6 paragraph limit.

9. Please sort the Materials Table alphabetically by the name of the material.

This has been done.

Point-by-point Response to Reviewer 1

Manuscript Summary:

The authors present a tutorial of cryo-SEM and cryo-FIB techniques and their application for energy materials with solid/liquid interfaces. This will be a good resource for those working in this field. I have no issues with the content of the work and believe it to be high quality and impactful.

Major Concerns: None

Minor Concerns:

1. The title at present seems overly broad, and may imply cryo-TEM to many readers. I would suggest the title to instead specify cryo-SEM/FIB so that the scope of the article is more clear.

The title has been revised to *“Nanoscale characterization of liquid-solid interfaces in energy devices by coupling cryo-FIB with scanning electron microscopy and spectroscopy”*

2. Figures 3 and 4 could use some annotations to make clear which layers are the Li and electrolyte. At present, it is not obvious to readers without some experience in interpreting FIB cross-sections of Li metal deposits.

We thank the reviewer for the suggestion. Figures depicting cross sections of lithium metal batteries have been annotated as suggested.

Point-by-point Response to Reviewer 2

Reviewer #2:

Manuscript Summary:

This manuscript represents cryogenic microscopy techniques that have been in development for many years and as such it will serve as an invaluable guide for many upcoming cryo-EM researchers, especially in the field of energy storage research. I have a few minor questions and

suggestions that I think should be addressed in the manuscript. The authors did a nice job of detailing the process and results and I recommend the manuscript for publication with very minor revisions.

Major Concerns: N/A

Minor Concerns:

Line 179, Should a user wait for thermal equilibration before imaging begins? If so, approximately how long?

We have not observed any evidence that samples warm enough to warrant intentionally waiting for the system to re-equilibrate. However, it takes a few minutes to complete the loading process (the transfer rod has to be retracted, vacuum valves have to be closed, the slush station needs to be either emptied or covered etc.) and get set up at the controls of the FIB, turn on both beams and move the stage into position. We have added the following comment to the manuscript:

“NOTE: the time required to set up to start imaging is usually sufficient to allow the sample to reach thermal equilibrium on the cryo-stage, especially if both stages in the prep-chamber and the SEM chamber are cooled to the same temperature and the transfer time of the shuttle from one stage to the other is minimized.”

Line 211, Do you recommend condensation and then curing over curing while condensing? Please elaborate on why or why not.

In response to this comment and those from reviewer 3, we have elaborated on this and added two citations, namely Hayles et al. (Ref. 25) and Schreiber et al. (Ref. 13), which discuss the development of this method and describe it in more detail. Much of the elaboration was too involved for the protocol and is placed in the discussion section, but we have added the following sentence to step 2.9.: “This should produce a uniform layer of uncured organometallic platinum, and the user can briefly image the sample surface to confirm even coverage.” The addition to the discussion section is as follows:

“FIB systems typically use an organometallic platinum gas to carry the platinum to the surface of the sample. Under cryogenic conditions this precursor condenses on the cold sample surface to form a non-conductive platinum-containing organic compound²⁷. A curing process during which the layer is exposed to the ion beam then releases the organic component, allowing a conductive platinum layer to form. This step is critical for high-quality results as the platinum both dissipates charge and mitigates gallium implantation^{13,27}. Orienting the sample so that the surface is normal to the GIS source is the best way to get a continuous layer, and the exact position will need to be adjusted for each system. FIB systems typically use an organometallic platinum gas to carry the platinum to the surface of the sample. Under cryogenic conditions this

precursor condenses on the cold sample surface to form a non-conductive platinum-containing organic compound²⁷. A curing process during which the layer is exposed to the ion beam then releases the organic component, allowing a conductive platinum layer to form. This step is critical for high-quality results as the platinum both dissipates charge and mitigates gallium implantation^{13,27}. Orienting the sample so that the surface is normal to the GIS source is the best way to get a continuous layer, and the exact position will need to be adjusted for each system. "

General question: I would assume that a battery/deposit would have a macroscope (hundreds of microns) electrolyte thickness but the electrolytes on the Li deposits look to be only a few microns in thickness, how is that thickness achieved? This may be useful information for users, especially since FIB milling is realistically limited to tens of microns sized features.

We have found that the electrolyte thickness varies widely between sample geometries. For example, a symmetric cell composed of two lithium foils and a membrane (celgard) separator will consistently produce an electrolyte layer a few microns thick after opening the cell and freezing in slush nitrogen, while a cell with an o-ring separator, a lithium foil on one electrode and a stainless steel substrate may produce an electrolyte layer hundreds of microns thick. The latter case was resolved by switching to a membrane separator. However, these observations are anecdotal, and users should adapt to their particular case.

Thank you for this question, as it inspired edits which will make the protocol more useful. Namely, we added to the discussion: *"Next, the technique is not immediately compatible with all sample geometries. For example, some battery samples tend to feature a thick electrolyte layer (30-100 μm) upon freezing which will require impractically long milling times when using a standard gallium ion FIB. Often slight modifications can be made to overcome this limitation. We have found that the electrolyte thickness can be reduced by switching from an O-ring separator to a membrane separator. However, the impacts of such modifications will vary between samples and should be done with careful consideration."*

General comment: The detection of Li is possible with EDS, but it is not straightforward for many EDS detectors. What detector was used for Li X-ray detection? Perhaps a small discussion on detecting Li would be beneficial. Please add the EDS detector model to the table of materials.

The reviewer is correct that detection of Li by EDX is not straight forward. The detector used in this work is an Oxford X-max 80 mm, which cannot practically be used to detect lithium. We have clarified this in the discussion section:

"While detection of lithium by EDX is possible²⁹, it requires the use of a detector specifically optimized for low energy X-rays which was not done in this work. More sensitive detectors will also improving the x-ray collection efficiency and thereby reduce the required electron dose for EDX mapping."

Point-by-point Response to Reviewer 3:

Reviewer #3:**Manuscript Summary:**

This manuscript describes a general protocol for the preparation and cross-sectional imaging and x-ray compositional analysis of cryogenically frozen specimens containing liquid/solid interfaces. The authors provide sufficient background in the introduction to motivate their contribution. The manuscript is divided into specific sections describing 1) cryogenic specimen preparation and transfer into the SEM instrument; 2) general SEM imaging to locate a region of interest; 3) FIB milling for cross-sectional imaging, and; 4) EDX compositional mapping. SEM image figures are presented which support the description of the protocol.

Major Concerns:

The presented figures only partially support the explained protocol, where additional figures and schematics are needed. Specifically:

* The last paragraph of the introduction describes the use of a "workstation with a 'slush pot'". This is followed by a convoluted description of freezing and transfer of specimens into the SEM chamber. Please include either an annotated photograph or a schematic describing the various parts/features (e.g. "slush pot"). Additionally, please be more explicit when describing the specimen shuttle suitcase transfer device. Many (if not most) readers will not have a clue about the Quorum system, so jargon like "prep" chamber, and the description of a "transfer rod featuring a small airlock" should be avoided to minimize confusion. For example, describing of the "transfer rod" is confusing; what I suspect you are trying to describe is the specimen shuttle suitcase device with an integrated air lock and transfer rod manipulator. Please be explicit. Again, an annotated picture of schematic would be helpful.

Thank you for pointing out that such a critical portion of the protocol was unclear. A new figure has been added as you have requested (figure 1 in the new version) as well as a short description in the text. All portions of the cryogenic system are shown with annotations. In addition, all jargon or imprecise language has been either eliminated or properly explained throughout the protocol. We hope that these edits make the protocol clearer.

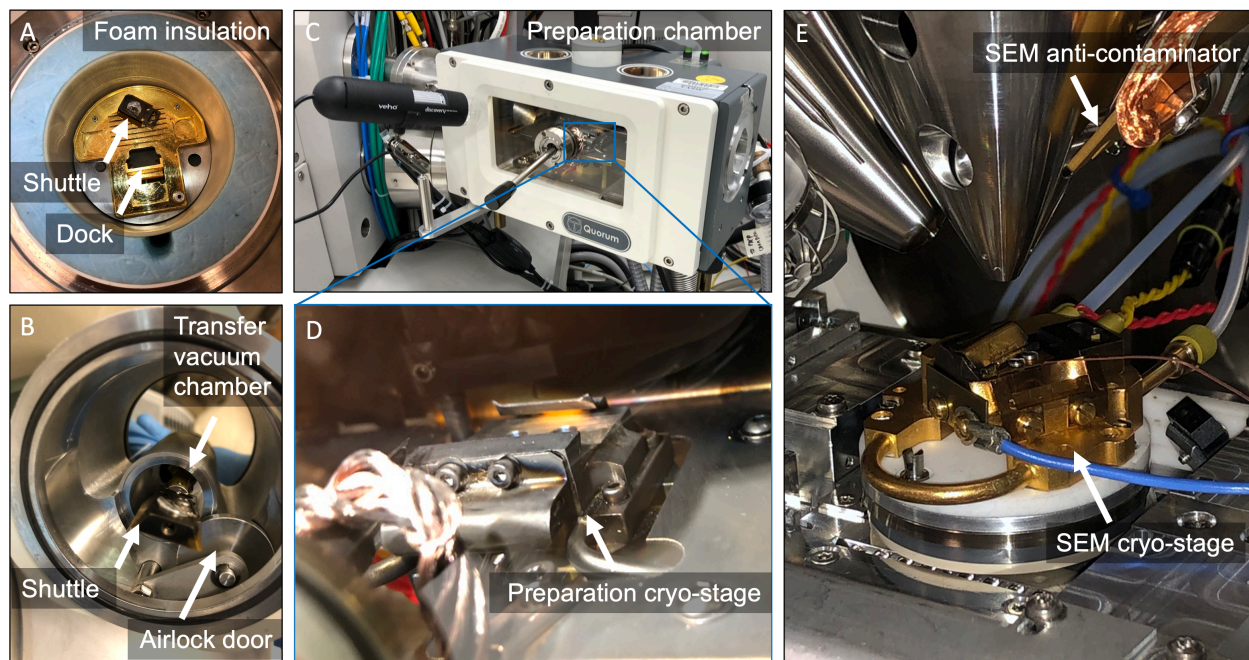


Figure 1: Components of the cryogenic FIB/SEM system used. (A) The slush pot for initial sample preparation. The main portion and a reservoir under the foam insulation are filled with liquid nitrogen, which is converted into slush nitrogen by reducing the pressure above the liquid nitrogen using a vacuum pump. Samples are plunge frozen in the slush nitrogen and attached to the shuttle before the vertical dock is used to lift the shuttle out on the transfer arm. **(B)** The inside of the transfer system. A small airlock holds the shuttle under weak vacuum during transfer to the preparation chamber, and the arm itself (not shown) allows users to move the sample onto the cryogenically cooled stage. **(C)** An outside view of the preparation chamber, where samples can be sputter-coated prior to imaging. **(D)** A closeup of the cryo-stage in the preparation chamber. **(E)** The cryo-system inside the SEM chamber, featuring the stage and the anticontaminator.

* Regarding section 3 (Prepare cross-sections), Please include a schematic illustration that describes the geometry, dimensions, and orientations of the specimen cuts relative to the beams and X-ray detector. Having to rely on the written description is quite challenging.

A figure has been added to this effect, and is the third figure in the revised draft.

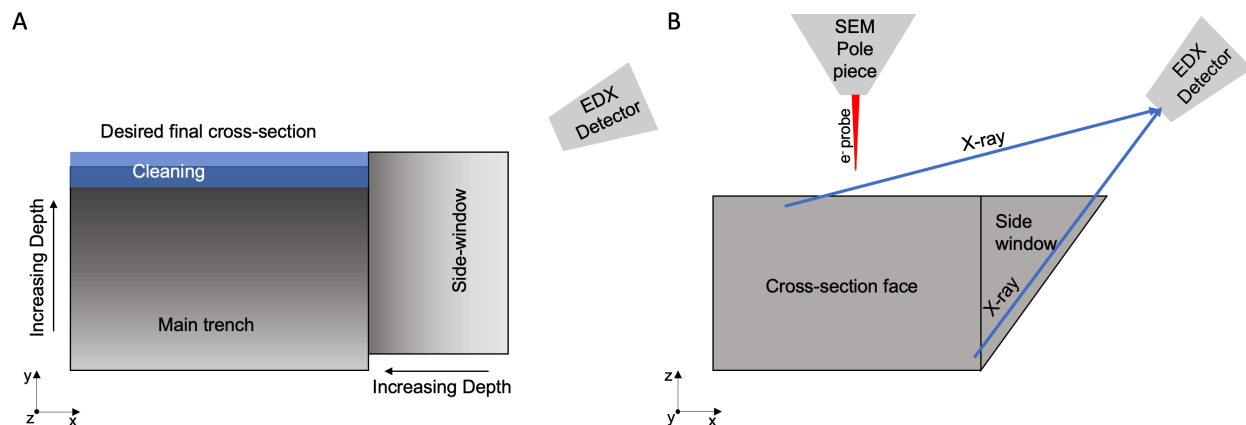


Figure 3: Setup of milling windows, including a side window for improved x-ray yield. (A) A schematic showing the key features of the milling process (placements are not exact). The main trench and side window are drawn showing the direction of increasing depth (indicated both by the labeled arrows and the gradient in shading), and the cleaning cross section (blue) is shown overlapping partially with the main trench. The side window is aligned relative to the position of the EDX detector to allow for detection of x-rays generated from the entire cross section. **(B)** A sketch demonstrating the benefit of the side window. As the electron probe scans the cross-section, electrons excite x-rays, which are measured by the EDX detector. Without a side window, shadow effects would result in parts of the cross-section (such as the bottom right here) to appear dark.

In the main text we have added: “For EDX experiments, the FIB milling geometry should be optimized and the position of the EDX detector should be taken into account as shown schematically in Figure 3. Fig. 3A depicts the milling setup viewed from the direction of the ion beam: A main trench and side window are created first, with the side window rotated clockwise 270 degrees to produce the desired depth gradient with respect to the position of the EDX detector. Subsequently, a cleaning cross section is milled (blue box in Fig. 3A) to create the final face of the cross section. The side window is milled at least 1 μm past the end of the original main trench so that the cleaning cross section will be at least flush with the side of this trench. The side window establishes a line of sight from each point in the cross-section to the detector (Fig. 3B).”

* Describe some of the limitations of the Quorum system, specifically lack of full rotation and how it affects the approach (maybe it doesn't affect it much).

Minor Concerns:

1. Line 50: please include after "energy devices" any recent relevant work by others, including the references below for corroded materials (Schreiber et al. 2018, Ultramicro 194, 89-99; Perea et al. 2020, npj Mater Degrad 4, 1-7; Li et al. 2020, Corr Sci 174, 108812).

The citations have been added.

2. Line 93: awkward use of hyphens. Consider using parentheses.

The hyphens were replaced with parentheses as suggested.

3. Line 105: provide statement about temperature control. You just say "held at liquid nitrogen temperature"

We have clarified that the stages should be held at -175°C throughout the protocol.

4. Line 105: Describe that metals other than Au-Pd can be sputter coated.

The line now reads *"...sputter coated with a conductive layer, such as a gold-palladium alloy."*

5. Lines 108-110: again having an annotated picture/schematic would be helpful in explaining this. Otherwise, those not familiar with the Quorum systems will not know what you are talking about. Consider that others may be using other cryo FIB/SEM systems by different companies.

As discussed above, we have followed the suggestion by the reviewer to provide details on our set up.

6. Lines 118-122: This is an important step. Provide more details as to how this is done in your specific case. I suspect since an FEI microscope is used, that this requires a loosening of the setscrew on the GIS, and clockwise rotation a specific number of turns. Please be explicit about this in your case and mention that this specific procedure may vary with different equipment.

We have added *"On the FEI Strata used here, this is done by loosening a set screw on the side of the GIS source and rotating the collar 3 turns clockwise."*

7. Line 128: Section 1.1.5 would benefit from having a section heading distinguishing "Set up the cryo prep station" from the above "set up the microscope"

This edit was made.

8. Line 131: provide more details as to what would be causing clogging. Might not be obvious to many.

The line has been edited to *“This flushes moisture out of the system to mitigate the formation of ice in the lines upon cooling, which can impede the flow of gas.”*

9. Line 138-140: again having a figure would be helpful for explaining this

See prior discussion of the added figures.

10. Line 155: again, the specimen shuttle suitcase device is not the "transfer rod"; it does have a transfer rod.

The term “transfer system” has been used to clarify this point.

11. Line 167: provide an estimated thickness of the Au-Pd film deposited using the described conditions

The step now reads: *“At this point, a ~5-10 nm thick gold-palladium layer can be sputtered onto the sample surface to mitigate charging. Typical starting values are 10 mA for 10 seconds, though these parameters should be adjusted for each system.”*

12. Line 211-212: Provide an expatiation of this step. This procedure is very important to provide sufficient protective cap and was first describe by Hayles et al (JOM, 226, 3 263-269, 2007) and then further explained by Schrieber et al. (Ultramicro, 194, 89-99, 2018) as 'curing' the film into a denser protective cap.

In the protocol we simply changed this step to include: *“This should produce a uniform layer of uncured organometallic platinum, and the user can briefly image the sample surface to confirm even coverage.”* However, we made extensive additions including both references to the discussion section to include details on this important step. The discussion now includes the following:

“FIB systems typically use an organometallic platinum gas to carry the platinum to the surface of the sample. Under cryogenic conditions this precursor condenses on the cold sample surface to form a non-conductive platinum-containing organic compound²⁷. A curing process during which the layer is exposed to the ion beam then releases the organic component, allowing a conductive platinum layer to form. This step is critical for high-quality results as the platinum both dissipates charge and mitigates gallium implantation^{13,27}. Orienting the sample so that the surface is normal to the GIS source is the best way to get a continuous layer, and the exact position will need to be adjusted for each system. FIB systems typically use an organometallic platinum gas to carry the platinum to the surface of the sample. Under cryogenic conditions this precursor condenses on the cold sample surface to form a non-conductive platinum-containing

organic compound²⁷. A curing process during which the layer is exposed to the ion beam then releases the organic component, allowing a conductive platinum layer to form. This step is critical for high-quality results as the platinum both dissipates charge and mitigates gallium implantation^{13,27}. Orienting the sample so that the surface is normal to the GIS source is the best way to get a continuous layer, and the exact position will need to be adjusted for each system. ”

13. Line 389: unclear as to what you are referring to.

In the submitted version line 389 mentioned changing the position of the side window, and we are interpreting this comment to mean that it was unclear why one would have to move the side window. Figure 3 and the accompanying discussion should clarify that the side window is used to establish a direct line of sight from every point on the cross section face, and that users should change the geometry of this trench as needed.

14. Line 424-436: again having a schematic to describe the trenching geometry would be helpful when trying to understand your description of windows.

[See the previous discussion of the figures.](#)

Point-by-point Response to Reviewer 4:

Reviewer #4:

Manuscript Summary:

The liquid/solid interface plays an essential role in various fields and a thorough atomic-level understanding of it is on demand. The cryo-SEM used in this manuscript shows higher efficiency in the preparation of samples than cryo-STEM, which requires ultra-thin samples. The vitrification can preserve the native state of interface and cryo-FIB can access the internal interfaces buried between two bulk phases. In addition, the chemical characterization is possible by EDX mapping. This technique shows good potential in characterizing the liquid/solid interface at nanoscale.

The protocols introduced in this manuscript about sample preparation, structural and chemical characterization are detailed and clear. The sample prepared and transferred according to the protocols can avoid crystallization and ice contamination to a great extent. Coating the sample initially with a thin layer of gold-palladium can minimize the effects of sample charging and radiation damage. However, there are some issues the authors need to clarify before the recommendation for publication.

Minor Concerns:

Figure 1 a, b in manuscript show a well-preserved sample and a less-preserved sample, while the protocols used to prepare these two samples haven't been mentioned. What are the factors leading to the difference? What's more, the authors claimed that one should insert the

sample into nitrogen quickly. This is a key step in vitrification. It would be good to quantify the cooling rate.

We added clarification that *“For Fig. 4, both samples were nominally prepared according to the same procedure, however, brief exposure to air most likely resulted in surface reactions for the sample in Fig. 4B possibly due to a thinner electrolyte layer on the surface of the lithium electrode. Screening of each sample after loading into the cryo-FIB helps identify potential issues due to the vitrification process.”* Additionally, the figure legend now says: *“The surface is far rougher, and deposits are not fully covered by electrolyte, suggesting sample reactions may have occurred due to prolonged air exposure during the preparation.”* The intention of the figure is to demonstrate the effects of doing this step incorrectly and clarify that users must evaluate each sample. Thank you for pointing out that this was not sufficiently clear.

Our setup does not allow for quantification of the cooling rate for individual samples. However, we have noted in the discussion of cryogens the increase in cooling rates when using liquid nitrogen vs. slush nitrogen: *“To prevent crystallization, slush nitrogen is used in this procedure, as it reduces the Leidenfrost effect and accelerates cooling compared to liquid nitrogen^{8,23,24}. We also note that compared to aqueous solutions many organic liquids require significantly lower cooling rates for vitrification^{25,26}, which is beneficial for freezing of thicker organic electrolyte layers.”*

Permissions for reuse of material for Figure 2 in the updated manuscript:

Dear Dr. Kourkoutis,

Your permission requested is granted and there is no fee for this reuse. In your planned reuse, you must cite the ACS article as the source, add this direct link <https://pubs.acs.org/doi/10.1021/acsenergylett.0c00202> and include a notice to readers that further permissions related to the material excerpted should be directed to the ACS.

If you need further assistance, please let me know.

Sincerely,
Simran Mehra
ACS Publications Support
Customer Services & Information
Website: <https://help.acs.org/>

Incident Information:

Incident #: 3752153
Date Created: 2020-08-18T07:03:26
Priority: 3
Customer: Lena Kourkoutis
Title: reuse of figure
Description: I am requesting permission to reuse the following figure from our ACS Energy Lett. Paper. Details are include below:

- A link to the ACS article from which you wish to reuse content:
<https://doi.org/10.1021/acsenergylett.0c00202>
- The portion of content you wish to reuse: Fig. 2
- A description of where the content will be reused: JoVE – video describing the methods introduced in our ACS Energy Letters paper

Thanks,
Lena F. Kourkoutis

Lena F. Kourkoutis, Associate Professor and Director of Undergraduate Studies
Rebecca Q. and James C. Morgan Sesquicentennial Faculty Fellow
Applied and Engineering Physics I Cornell University
235 Clark Hall | Ithaca, NY 14853 | USA

Permissions for reuse of material for Figure 7 in the updated manuscript:

**CAMBRIDGE UNIVERSITY PRESS LICENSE
TERMS AND CONDITIONS**

Nov 03, 2020

This Agreement between Lena F Kourkoutis ("You") and Cambridge University Press ("Cambridge University Press") consists of your license details and the terms and conditions provided by Cambridge University Press and Copyright Clearance Center.

License Number	4891660302447
License date	Aug 17, 2020
Licensed Content Publisher	Cambridge University Press
Licensed Content Publication	Microscopy and Microanalysis
Licensed Content Title	Site-Specific Preparation of Intact Solid–Liquid Interfaces by Label-Free In Situ Localization and Cryo-Focused Ion Beam Lift-Out
Licensed Content Author	Michael J. Zachman, Emily Asenath-Smith, Lara A. Estroff, Lena F. Kourkoutis
Licensed Content Date	Nov 21, 2016
Licensed Content Volume	22
Licensed Content Issue	6
Start page	1338
End page	1349
Type of Use	Journal/Magazine

Requestor type	Author
Requestor details	Not-for-profit
Format	Electronic
Portion	Figure/table
Number of figures/tables	1
Author of this Cambridge University Press article	Yes
Author / editor of the new work	Yes
Title of new article	Nanoscale characterization of liquid-solid interfaces in energy devices by cryogenic-electron microscopy
Lead author	Taylor Moon
Title of targeted journal	JoVE
Publisher	MyJove Corp
Expected publication date	Dec 2020
Portions	Fig. 6
Territory for reuse	World
If publisher of new journal/magazine has its main base in USA, Canada or Mexico	No
Requestor Location	Lena F Kourkoutis 212 Clark Hall Cornell University Ithaca, NY 14853 United States Attn: Lena F Kourkoutis

Publisher Tax ID

GB823847609

Total

0.00 USD

Terms and Conditions

TERMS & CONDITIONS

Cambridge University Press grants the Licensee permission on a non-exclusive non-transferable basis to reproduce, make available or otherwise use the Licensed content 'Content' in the named territory 'Territory' for the purpose listed 'the Use' on Page 1 of this Agreement subject to the following terms and conditions.

1. The License is limited to the permission granted and the Content detailed herein and does not extend to any other permission or content.
2. Cambridge gives no warranty or indemnity in respect of any third-party copyright material included in the Content, for which the Licensee should seek separate permission clearance.
3. The integrity of the Content must be ensured.
4. The License does extend to any edition published specifically for the use of handicapped or reading-impaired individuals.
5. The Licensee shall provide a prominent acknowledgement in the following format: author/s, title of article, name of journal, volume number, issue number, page references, , reproduced with permission.

Other terms and conditions:

v1.0

Questions? customercare@copyright.com or +1-855-239-3415 (toll free in the US) or +1-978-646-2777.